sciendo

Polish Journal of Chemical Technology, 20, 2, 32—39, 10.2478/pjct-2018-0020

Batch removal of Pb (II) ions from aqueous medium using gamma-Al_2O_3 nanoparticles/ethyl cellulose adsorbent fabricated via electrospinning method: An equilibrium isotherm and characterization study

Ehsan Sadeghi Pouya, Hooman Fatoorehchi*, Mohammad Foroughi-Dahr

School of Chemical Engineering, College of Engineering, University of Tehran, P.O. Box, 1365-4563, Tehran, Iran
**Corresponding author: e-mail: hfatoorehchi@ut.ac.ir, hfatoorehchi@gmail.com*

The aim of the present work is to study the efficiency of a biocompatible polymer-based adsorbent for the removal of Pb (II) ions whose devastating effects on people's health is a matter of great concern from aqueous solution. In this study, ethyl cellulose and gamma-Al_2O_3 nanoparticles/ethyl cellulose electrospun adsorbents were prepared for the batch removal of Pb (II) ions from aqueous solution. Both samples were characterized using contact angle analysis, N_2 adsorption/desorption technique, FT-IR and SEM. The Freundlich model (R-square = 0.935 and RMSD (%) = 6.659) and the Dubinin-Radushkevich model (R-square = 0.944 and RMSD (%) = 6.145) were found to be more reliable in predicting the experimental data from the adsorption of Pb (II) ions onto the electrospun gamma-Al_2O_3 nanoparticles/ethyl cellulose than the Langmuir model (R-square = 0.685 and RMSD (%) = 14.61) and also the Temkin model (R-square = 0.695 and RMSD (%) = 14.38).

Keywords: Adsorption; Pb (II) ions; Ethyl cellulose; Gamma-Al_2O_3 nanoparticles; Electrospinning.

INTRODUCTION

Nowadays, the profoundly adverse impact of poor water quality on people's health has become a cause for growing concern in almost all countries in the developing world. Among all contaminants discharged into the environment, heavy metals are categorized as one of the most hazardous ones, even in very low concentrations. According to the World Health Organization, the exposure to a concentration of Pb (II) ions higher than 0.01 mg/L in potable water can irreversibly damage different bodily functions[1–4]. Pb (II) ions can be found in the effluent of a diverse range of industrial sectors, including the production of dyes and pigments, glassware, alloys, batteries, electronic equipment etc[5, 6].

Adsorption is considered to be a highly reliable method in order to treat wastewaters containing heavy metals, mainly due to its low cost and high flexibility in design and operation, high selectivity and also high regeneration capacity[7–10]. Among the researches into the synthesis of efficient adsorbents in recent years[7–12], agro-based waste materials[12], activated carbons[13] and minerals[14] are so popular adsorbents. Over the past few years, sheet-like adsorbents has attracted much attention mostly because they are much easier than powder-like adsorbents for being separated from the liquid phase and for being recovered after the process[15, 16]. Polymers are among the most common compounds in the preparation of sheet-like adsorbents. Compared with several other techniques, electrospinning is considered to be a simple technique which allows the mass production of highly porous, interconnected sheet-like adsorbents[17–20].

Many polymers have shown considerable potential for being electrospun thus far[18]. In order to prepare materials used for environmental purposes like the treatment of wastewaters, ethyl cellulose can serve as a promising candidate since it is classified as a biocompatible polymer[21]. For increasing the efficiency of polymeric adsorbents in the removal of metal ions from aqueous medium, metal oxide nanoparticles are popular modifying agents because of their high surface area and also their surface hydroxyl groups[22–29]. Al_2O_3 nanoparticles are a common type of metal oxide nanoparticles which are well-known for the absence of diffusion resistance in their internal structure, their high surface binding energy and their considerable ability to increase the water permeability of the matrix into which they are impregnated[30, 31]. These characteristics make Al_2O_3 nanoparticles appropriate for being used as modifying agents in the preparation of adsorbents for purifying aqueous systems.

In the present work, ethyl cellulose and gamma- Al_2O_3 nanoparticles-modified ethyl cellulose adsorbents were prepared by means of electrospinning method for the batch removal of Pb (II) ions from aqueous solution. The prepared samples were characterized using contact angle analysis, N_2 adsorption/desorption technique, Fourier transform infrared spectroscopy and scanning electron microscopy. The equilibrium adsorption isotherm was experimentally obtained for the adsorption of Pb (II) ions onto the electrospun gamma-Al_2O_3 nanoparticles/ethyl cellulose and the data were fitted to the Langmuir, Freundlich, Dubinin-Radushkevich and Temkin isotherm models.

MATERIALS AND METHODS

Materials

Ethyl cellulose (with an ethoxyl content of 48% and an average molecular weight of 100.000 g/mol), ethanol (with a purity of 99.7%) and gamma-Al_2O_3 nanoparticles (with a purity of 99.99%) were purchased from the Exir company, the Merck company and the TECNAN company, respectively. Table 1 lists the morphology, the BET surface area, the total pore volume and the average pore diameter of the gamma-Al_2O_3 nanoparticles, according to the datasheet provided by the company. Anhydrous Pb (II) nitrate (with an analytical grade) from the Merck company was used as the source of Pb (II) ions in this study. All chemicals were used without any further purification.

Table 1. The morphology, the BET surface area, the total pore volume and the average pore diameter of the gamma-Al_2O_3 nanoparticles

Morphology	Average particle size [nm]	BET surface area [m^2/g]	Total pore volume [cm^3/g]	Average pore diameter [nm]
Spherical	10 – 20	90 –160	0.391	13.36

Adsorbent preparation and characterization

In order to prepare electrospinning solutions, ethyl cellulose (10 g) was initially dissolved in ethanol (50 mL) using a magnetic stirrer. The stirring process was carried out at ambient temperature (around 25°C) for 2 h. The gamma-Al_2O_3 nanoparticles/ethyl cellulose solution was also prepared by dispersing the nanoparticles (1 g) in the ethyl cellulose solution (10 mL) using an ultrasonic probe dispersion equipment. The dispersing process was carried out at 10 kHz for 30 min.

The electrospinning equipment used in this study is schematically shown in Fig. 1. As can be seen, the main parts of the electrospinning equipment were a syringe pump (for pumping out the polymeric solution loaded into a syringe), a DC high voltage power supply connected to the tip of the syringe needle (for electrically charging the polymeric solution being pumped out) and a rotating cylindrical collector wrapped in aluminium foil (for collecting fibers). In the electrospinning process, the solution was first loaded into a 5-mL plastic syringe equipped with a 22-gauge steel needle with a length of 3 cm. The syringe was then located in the syringe pump working at 1 mL/h. The distance between the needle tip and the collector was also fixed at 10 cm. The voltage at which both ethyl cellulose and gamma-Al_2O_3 nanoparticles/ethyl cellulose solutions were electrospun was 10 kV. The Taylor equation (Eq. (1)) can be used to calculate the minimum voltage, which is known as critical voltage, needed for overcoming the surface tension of the solution and initiating the electrospinning process[32, 33]:

$$V_c^2 = \frac{4H^2}{L^2}\left(\ln\frac{4L}{D} - 1.5\right)(0.058\pi D\gamma) \quad (1)$$

In Eq. (1), V_c (kV) is the critical voltage, H (cm) is the needle tip-collector separation distance, L (cm) is the length of the needle, D (cm) is the internal diameter of the needle and γ (mN/m) is the surface tension of the solution. The surface tension of both ethyl cellulose and gamma-Al_2O_3 nanoparticles/ethyl cellulose solutions was measured using a force tensiometer (Krüss, K6) and found to be approximately 34.5 mN/m. Using Eq. (1), the value of V_c in this study was found to be just above 7 kV.

The static water contact angle analysis was performed using a video-based optical contact angle measuring instrument (Dataphysics, OCA 15 Plus) for comparing the electrospun ethyl cellulose and gamma-Al_2O_3 nanoparticles/ethyl cellulose in terms of water permeability. The measurement was made by taking a photograph of the shape of a water droplet after being positioned for 5 s on the surface of each sample. The BET surface area, total pore volume and average pore diameter of the samples were measured by the N_2 adsorption/desorption technique at –196°C using a gas adsorption analyzer (BEL Japan, BELSORP-mini II). Prior to the analysis, the samples were degassed under a flow of air with a temperature of 120°C for 2 h. The functional groups existing on the surface of the samples were compared by the Fourier transform infrared (FT-IR) spectroscopy in the range of 4000–400 cm^{-1} using a spectrometer (Bruker, Tensor 27). The surface morphology of the samples was also studied by the scanning electron microscopy (SEM) analysis using an electron microscope (TESCAN, MIRA3).

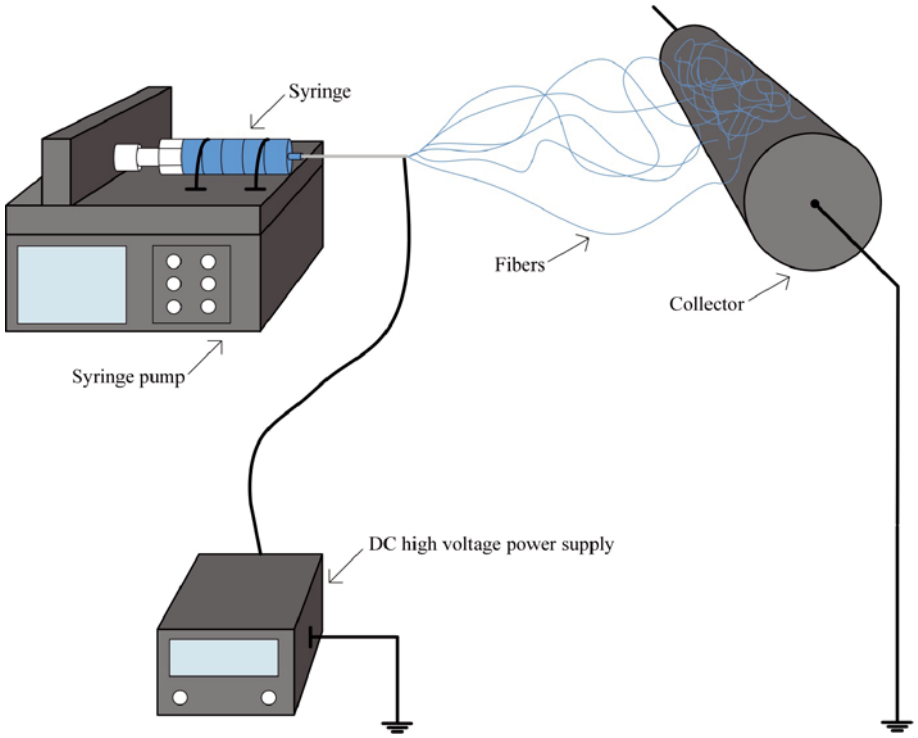

Figure 1. The scheme of the electrospinning equipment

Batch adsorption study

Adsorption experiments were conducted by contacting the adsorbent (0.1 g) with aqueous solutions containing Pb (II) ions (50 mL) at five different initial concentrations (50, 100, 150, 200 and 250 mg/L) in a series of 100-mL Erlenmeyer flasks. The flasks were shaken at 200 rpm and at 25°C in a thermostatic shaking incubator for 24 h. It should be noted that the initial pH value of solutions was not adjusted. After 24 h, the adsorbent was separated from the liquid phase by a piece of filter paper and the remaining concentration of Pb (II) ions was subsequently measured using a flame atomic absorption spectrometer (Shimadzu, AA-670). The equilibrium capacity of the adsorbent at each initial concentration of Pb (II) ions can be calculated as below:

$$\text{Equilibrium adsporption effciency } (\%) = \frac{(C_0 - C_e)}{C_0} \times 100 \quad (2)$$

$$q_e = \frac{(C_0 - C_e)V}{M} \quad (3)$$

In Eqs. (1) and (2), C_0 (mg/L) is the initial concentration of Pb (II) ions, C_e (mg/L) is the equilibrium concentration of Pb (II) ions, q_e (mg/g) is the equilibrium adsorption capacity, V (L) is the solution and M (g) is the mass of the adsorbent used.

RESULTS AND DISCUSSION

Equilibrium adsorption isotherm

Our preliminary experiments indicated that the adsorption capacity of the electrospun ethyl cellulose fibers for the removal of Pb (II) ions from aqueous solution, compared to that of the electrospun gamma-Al_2O_3 nanoparticles/ethyl cellulose, is too low. In fact, our studies showed that, under the conditions mentioned earlier, the equilibrium capacity of the electrospun gamma-Al_2O_3 ranges between 1.030 and 6.013 mg/g with the increase in the initial concentration of Pb (II) ions from 50 to 250 mg/L, while the equilibrium capacity of the electrospun gamma-Al_2O_3 nanoparticles/ethyl cellulose lies in the range of 9.385–62.05 mg/g with the increase in the initial concentration of Pb (II) ions from 50 to 250 mg/L. Accordingly, the equilibrium adsorption isotherm studies were just carried out by the electrospun gamma-Al_2O_3 nanoparticles/ethyl cellulose. Figure 2 illustrates the effect of the initial concentration of Pb (II) ions on the equilibrium adsorption efficiency. Since both numerator and denominator in Eq. (1) change as the initial concentration changes, there is not any rational relationship between the values of the equilibrium adsorption efficiency and the values of the initial concentration.

The experimental data were fitted to the Langmuir, Freundlich, Dubinin-Radushkevich and Temkin isotherm models (Eqs. (3)–(6), respectively)[34]:

$$q_e = \frac{q_L K_L C_e}{1 + K_L C_e} \quad (4)$$

$$q_e = K_F C_e^{1/n_F} \quad (5)$$

$$q_e = q_{D\text{-}R} \exp\left(-K_{D\text{-}R} \left[R_g T \ln(1 + \frac{1}{C_e}) \right]^2 \right) \quad (6)$$

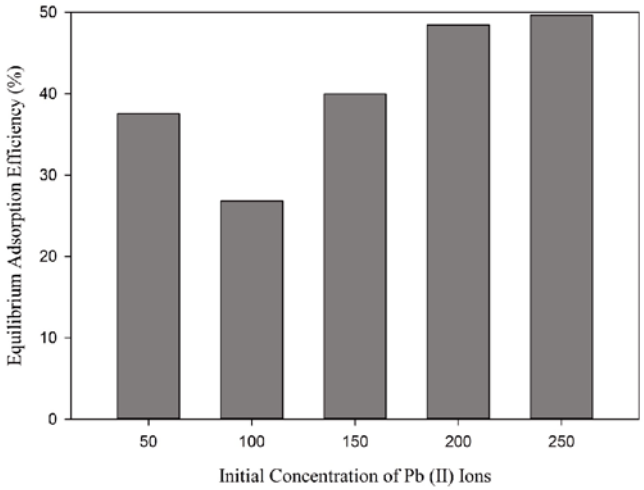

Figure 2. The effect of the initial concentration of Pb (II) ions on the equilibrium adsorption efficiency

$$q_e = \frac{R_g T}{b_T} \ln(A_T C_e) \quad (7)$$

In equations above, q_e (mg/g) is the equilibrium adsorption capacity, C_e (mg/L) is the equilibrium concentration of Pb (II) ions, q_L (mg/g) is the Langmuir adsorption capacity, K_L (L/mg) is the Langmuir isotherm constant, K_F (mg$^{(1-1/nF)}$ L$^{(1/nF)}$/g) is the Freundlich isotherm constant, n_F is the Freundlich isotherm intensity, $q_{D\text{-}R}$ (mg/g) is the Dubinin-Radushkevich adsorption capacity, $K_{D\text{-}R}$ (mol^2/kJ^2) is the Dubinin-Radushkevich isotherm constant, b_T (kJ/mol) is the Temkin isotherm constant, A_T (L/mg), Rg (8.314 J/mol K) is the universal gas constant and T (K) is the absolute temperature.

Figure 3 illustrates the experimental adsorption data and also the equilibrium isotherms predicted by the above-mentioned models. As Fig. 3 shows, the equilibrium adsorption capacity is directly proportional to the initial concentration of Pb (II) ions. To restate, the equilibrium adsorption increases as the initial concentration increases, which is due to the increase in the mass driving force in the adsorption medium as the initial concentration increases. The mass driving force increases as the difference between the concentration of adsorbate species in the solution and those removed increases. The rise in the

Isotherm model	Isotherm model and statistical parameters
Langmuir	q_L [mg/g] = 195.0 K_L [L/mg] = 0.003 R-square = 0.685 RMSD [%] = 14.61
Freundlich	K_F [L$^{2.148}$/mg$^{1.148}$ g] = 0.002 n_F = 0.466 R-square = 0.935 RMSD [%] = 6.659
Dubinin-Radushkevich	$q_{D\text{-}R}$ [mg/g] = 134.5 $K_{D\text{-}R}$ [mol^2/kJ^2] = 1.610E+4 R-square = 0.944 RMSD [%] = 6.145
Temkin	A_T [L/mg] = 0.033 b_T [kJ/mol] = 0.071 R-square = 0.695 RMSD [%] = 14.38

Table 2. The adjustable parameters, R-square values and RMSD percentages for the adsorption of Pb (II) ions from aqueous solution onto the electrospun gamma-Al_2O_3 nanoparticles/ethyl cellulose

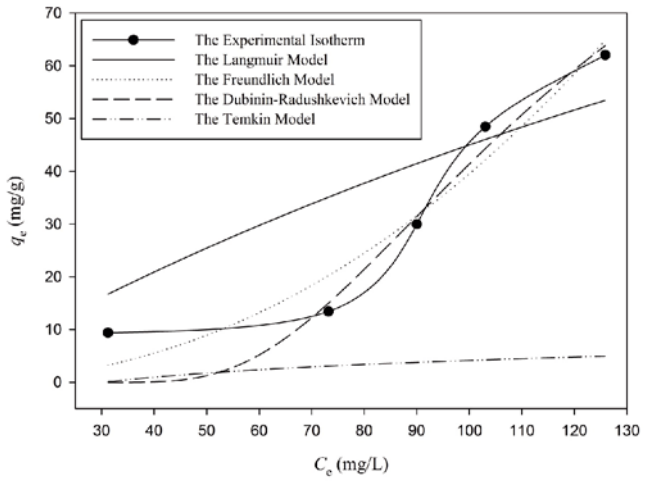

Figure 3. The equilibrium data and theoretical isotherms for the adsorption of Pb (II) ions from aqueous solution onto the electrospun gamma-Al_2O_3 nanoparticles/ethyl cellulose

mass driving force allows more Pb (II) ions to diffuse from the liquid phase into adsorbent structure, leading to higher adsorption capacities[35]. According to Alberti et al.[36], the experimental isotherm obtained in this study is phenomenologically categorized as a sigmoidal-shaped isotherm. This implies that the activation energy for the desorption of adsorbate species is concentration-dependent[37]. Table 2 lists the adjustable parameters for each model, R-square values and root mean square deviation (RMSD) percentages calculated by the MATLAB non-linear least squares optimization routine. As the tabulated results show, the Freundlich and Dubinin-Radushkevich models with higher R-square values and lower RMSD percentages much better fit the experimental data than the two other models.

The value of n_F can represent the extent to which an adsorption process is favourable. In general, an adsorbent has good adsorption characteristics when n_F is higher than unity[38]. Since n_F was found to be 0.466 in the present study, it can be argued that the electrospun gamma-Al_2O_3 nanoparticles/ethyl cellulose is not a highly efficient adsorbent for the removal of Pb (II) ions from aqueous solution, however, being much more efficient than ethyl cellulose fibers.

Using the following equation, one can also calculate the value of mean free energy in an adsorption process (E (kJ/mol)), which is defined as the energy needed for removing each adsorbate species from its location to infinity[34]:

$$E = \frac{1}{\sqrt{2K_{D\text{-}R}}} \tag{8}$$

The value of E lies between 8 and 16 kJ/mol when chemisorption dominates the process, while it is lower than 8 kJ/mol when physisorption is dominant. In the present study, the value of E is approximately 0.003 kJ/mol. This suggests that the adsorption of Pb (II) ions from aqueous solution onto the electrospun gamma-Al_2O_3 nanoparticles/ethyl cellulose occurs physically[39]. Table 3 lists the adsorption capacity of the electrospun gamma-Al_2O_3 nanoparticles/ethyl cellulose for the removal of Pb (II) ions from aqueous solution based on the Dubinin-Radushkevich model with that of some other adsorbents used in earlier researches in recent years[40–47].

Adsorbent	Adsorption capacity [mg/g]
Magnesium silicate impregnated palm-shell waste powdered activated carbon [40]	391.3
Triphosphate-modified waste Lyocell fibers [41]	367.6 ± 8.5
Chromium (III)-pillared copper-exchanged montmorillonite [42]	222.22
Gamma-Al_2O_3 nanoparticles [43]	217.39
Gamma-Al_2O_3 nanoparticles/ethyl cellulose (the present work)	134.5
Nanochitosan/sodium alginate/microcrystalline cellulose beads [44]	114.47
Biochar-supported reduced graphene oxide composite [45]	34.015
Coffee grounds [46]	22.9
Cerium dioxide nanoparticles [47]	4.995

Table 3. The adsorption capacity of the electrospun gamma-Al_2O_3 nanoparticles/ethyl cellulose and some other adsorbents used in other studies for the removal of Pb (II) ions from aqueous solution

Characterization studies

Figures 4 (A) and (B) illustrate the contact angle between a droplet of water and the surface of the electrospun ethyl cellulose fibers and gamma-Al_2O_3 nanoparticles/ethyl cellulose, respectively. As can be seen, adding gamma-Al_2O_3 nanoparticles to the ethyl

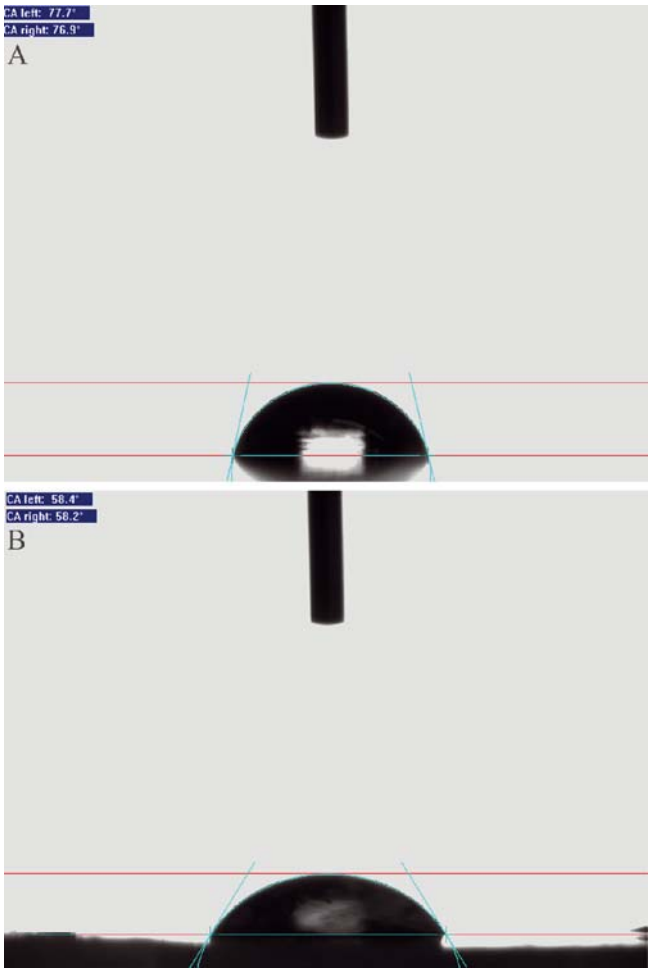

Figure 4. The contact angle between a water droplet and the surface of: (A) the electrospun ethyl cellulose and (B) the electrospun gamma-Al_2O_3 nanoparticles/ethyl cellulose

cellulose solution decreases the contact angle of the fabricated sample by about 19 degrees. By definition, the higher the contact angle, the more permeable the sample is to water. Therefore, the electrospun gamma--Al_2O_3 nanoparticles/ethyl cellulose is more permeable to water, thereby being more efficient for the adsorption of Pb (II) ions from aqueous solution.

Figures 5 (A) and (B) illustrate the N_2 adsorption/desorption isotherm and the BJH pore size distribution for the electrospun ethyl cellulose fibers and gamma--Al_2O_3 nanoparticles/ethyl cellulose, respectively. According to Sing et al.[48], both samples exhibit type III isotherms (convex to the relative pressure axis) which are characteristic of mesoporous adsorbents[49, 50]. The pore size distribution of the electrospun gamma-Al_2O_3 nanoparticles/ethyl cellulose reveals that pores in this sample are distributed less broadly (or more uniformly in size) than those in the electrospun ethyl cellulose[51–53]. The BET surface area, total pore volume and average pore diameter of each sample are given in Table 4. It is obvious that adding gamma-Al_2O_3 nanoparticles to the ethyl cellulose solution increases the BET surface area, total pore volume and average pore diameter of the fabricated sample.

Figure 6 displays the FT-IR spectrum of the electrospun ethyl cellulose and gamma-Al_2O_3 nanoparticles/ethyl cellulose and also gamma-Al_2O_3 nanoparticles. The absorption bands at about 3400 and 1600 cm^{-1} observed

Table 4. The BET surface area, total pore volume and average pore diameter of the electrospun ethyl cellulose and gamma-Al_2O_3 nanoparticles/ethyl cellulose

Sample	BET surface area [m^2/g]	Total pore volume [cm^3/g]	Average pore diameter [nm]
Ethyl cellulose fibers	6.279	0.010	6.785
Gamma-alumina nanoparticles/ethyl cellulose fibers	24.42	0.111	18.23

in the FT-IR spectrum of gamma-Al_2O_3 nanoparticles correspond to stretching and bending vibrations of –OH groups, respectively[54, 55]. As mentioned earlier in the introduction, the main mechanism in the adsorption of Pb (II) ions onto the electrospun gamma-Al_2O_3 nanoparticles/ethyl cellulose is thought to be the attraction between surface –OH groups and Pb (II) ions in the liquid phase. As Fig. 5 (B) depicts, these bands also exist on the surface of the electrospun gamma-Al_2O_3 nanoparticles/ethyl cellulose, however they overlap similar bands in the FT-IR spectrum of the electrospun ethyl cellulose. The peak at about 3400 cm^{-1} in the FT-IR spectrum of the electrospun ethyl cellulose is associated with intra and/or intermolecular vibrations of –OH groups on the chains of ethyl cellulose, while the peak at 1600 cm^{-1} results from C=O and C=C stretching vibrations[56, 57].

The SEM images of the electrospun ethyl cellulose and gamma-Al_2O_3 nanoparticles/ethyl cellulose are displayed

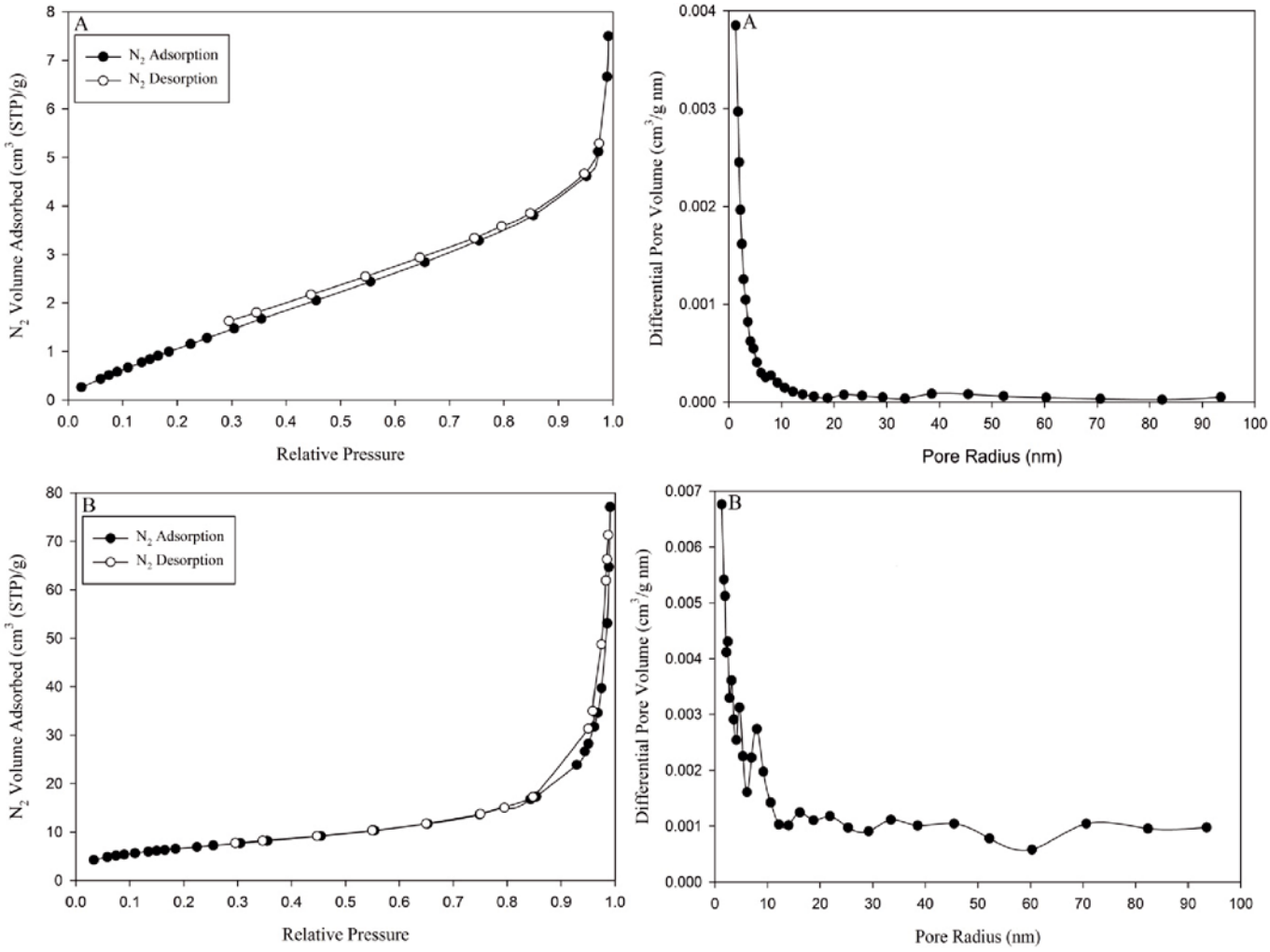

Figure 5. The N_2 adsorption/desorption isotherm (on the left) and the BJH pore size distribution (on the right) of: (A) the electrospun ethyl cellulose and (B) the electrospun gamma-Al_2O_3 nanoparticles/ethyl cellulose

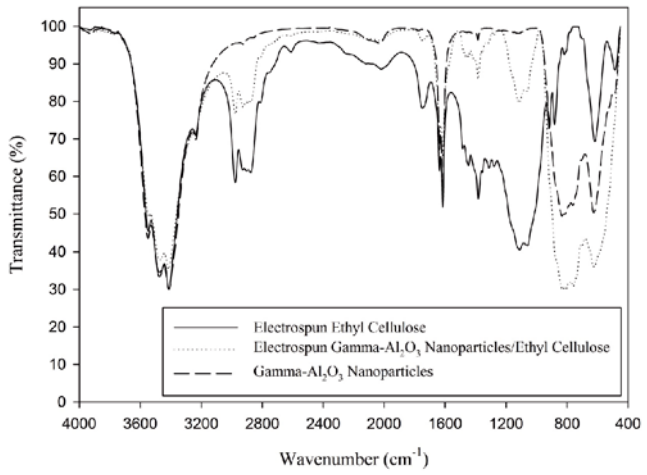

Figure 6. The FT-IR spectra of the electrospun ethyl cellulose, the electrospun gamma-Al_2O_3 nanoparticles/ethyl cellulose and gamma-Al_2O_3 nanoparticles

in Fig. 7 at three different magnification levels (500 x, 5.00 kx and 10.0 kx). From Fig. 7, it is clear that the morphology of the electrospun ethyl cellulose significantly different from that of the electrospun gamma-Al_2O_3 nanoparticles/ethyl cellulose. Indeed, the electrospun ethyl cellulose has a fibrous morphology, while the surface of the electrospun gamma-Al_2O_3 nanoparticles/ethyl cellulose is irregular in shape.

CONCLUSIONS

In the present work, ethyl cellulose, as a biocompatible polymer, was used in order to prepare an efficient adsorbent via electrospinning method for the batch removal of Pb (II) ions, one of the most hazardous contaminants for human health, from aqueous solution. Adding gamma-Al_2O_3 nanoparticles to the ethyl cellulose electrospinning solution showed a remarkable increase in the adsorption capacity of the prepared adsorbent for the removal of Pb (II) ions. This shows that these nanoparticles might be useful in the preparation of other types of polymeric adsorbents and membranes used for the removal of heavy metal ions or other pollutants which are ionized into positive form in aqueous medium. The electrospun gamm-Al_2O_3 nanoparticles/ethyl cellulose with a relatively high adsorption capacity compared with other adsorbents which need complex procedures to be prepared can be used as membranes in purifying wastewaters in both batchwise and continuous modes. The adsorbent prepared in this study might also be used as the substrate for preparing adsorbents which can be used in adsorption/photocatalytic hybrid separation processes after being modified by photocatalytic nanostructured materials

CONFLICT OF INTEREST

The authors have no conflicts of interest to declare.

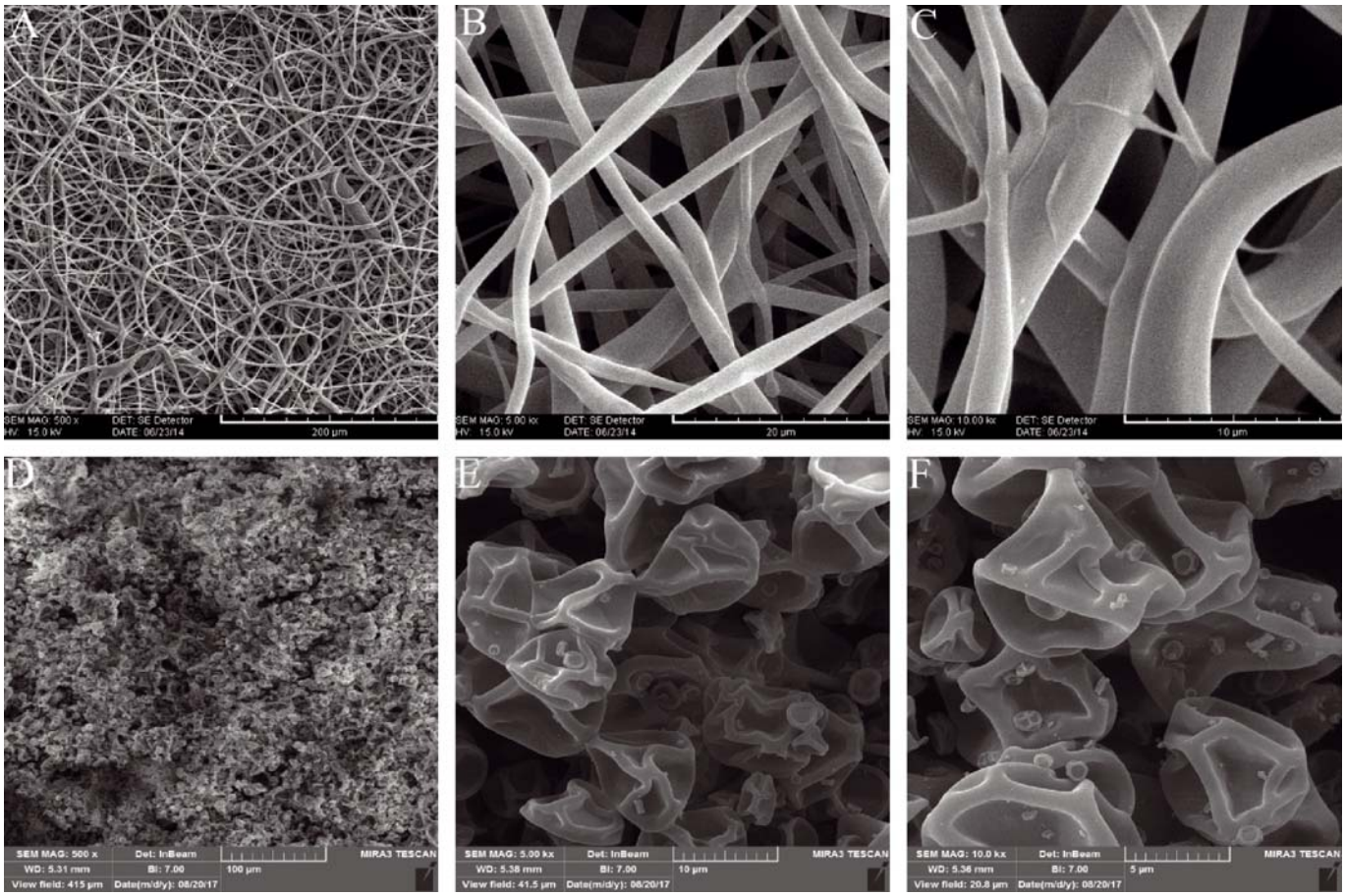

Figure 7. The SEM images of: (A, B and C) the electrospun ethyl cellulose (500 x, 5.00 kx and 10.0 kx) and (D, E and F) the electrospun gamma-Al_2O_3 nanoparticles/ethyl cellulose (500 x, 5.00 kx and 10.0 kx)

ACKNOWLEDGEMENTS

The authors are sincerely grateful to the editors and the anonymous reviewers of the journal of Polish Journal of Chemical Technology for their insightful comments and suggestions. The Pharmaceutical Sciences Research Center, Pharmaceutical Sciences Branch, Islamic Azad University, Tehran, Iran and the Laboratory for Instrumental Analysis, School of Chemical Engineering, College of Engineering, University of Tehran, Tehran, Iran are greatly acknowledged for their kind help and support in this study.

LITERATURE CITED

1. Singha, B. & Das, S.K. Removal of Pb(II) ions from aqueous solution and industrial effluent using natural biosorbents. *Environ. Sci. Pollut. Res*. 19 (2012) 2212–2226. DOI: 10.1007/s11356-011-0725-8.

2. Yang, R., Aubrecht, K.B., Ma, H., Wang, R., Grubbs, R.B., Hsiao, B.S. & Chu, B. Thiol-modified cellulose nanofibrous composite membranes for chromium (VI) and lead (II) adsorption, Polym. (United Kingdom). 55 (2014) 1167–1176. DOI: 10.1016/j.polymer.2014.01.043.

3. Pfadenhauer, L.M., Burns, J., Rohwer, A. & Rehfuess, E.A. Effectiveness of interventions to reduce exposure to lead through consumer products and drinking water: A systematic review. *Environ. Res*. 147 (2016) 525–536. DOI: 10.1016/j.envres.2016.03.004.

4. Klapiszewski, Ł. & Szatkowski, T. Removal of lead (II) ions by an adsorption process with the use of an advanced SiO_2 / lignin biosorbent. *Polish J. Chem. Technol.* 19 (2017) 48–53. DOI: 10.1515/pjct-2017-0007.

5. Pitsari, S., Tsoufakis, E. & Loizidou, M. Enhanced lead adsorption by unbleached newspaper pulp modified with citric acid. *Chem. Eng. J*. 223 (2013) 18–30. DOI: 10.1016/j.cej.2013.02.105.

6. Bensacia, N., Fechete, I., Moulay, S., Hulea, O., Boos, A. & Garin, F., Kinetic and equilibrium studies of lead(II) adsorption from aqueous media by KIT-6 mesoporous silica functionalized with -COOH, Comptes Rendus Chim. 17 (2014) 869–880. DOI: 10.1016/j.crci.2014.03.007.

7. Fu, F. & Wang, Q. Removal of heavy metal ions from wastewaters: A review. *J. Environ. Manage.* 92 (2011) 407–418. DOI: 10.1016/j.jenvman.2010.11.011.

8. Carolin, C.F., Kumar, P.S., Saravanan, A., Joshiba, G.J. & Naushad, M., Efficient techniques for the removal of toxic heavy metals from aquatic environment: A review. *J. Environ. Chem. Eng*. 5 (2017) 2782–2799. DOI: 10.1016/j.jece.2017.05.029.

9. Burakov, A.E., Galunin, E.V., Burakova, I.V., Kucherova, A.E., Agarwal, S., Tkachev, A.G. & Gupta, V.K. Adsorption of heavy metals on conventional and nanostructured materials for wastewater treatment purposes: A review, Ecotoxicol. Environ. Saf. 148 (2018) 702–712. DOI: 10.1016/j.ecoenv.2017.11.034.

10. Peng, W., Li, H., Liu, Y. & Song, S. A review on heavy metal ions adsorption from water by graphene oxide and its composites. *J. Mol. Liq*. 230 (2017) 496–504. DOI: 10.1016/j.molliq.2017.01.064.

11. Bhattacharyya, K.G. & Sen Gupta, S. Adsorption of a few heavy metals on natural and modified kaolinite and montmorillonite: A review. *Adv. Colloid Interface Sci.* 140 (2008) 114–131. DOI: 10.1016/j.cis.2007.12.008.

12. Demirbas, A., Heavy metal adsorption onto agro-based waste materials: A review. *J. Hazard. Mater*. 157 (2008) 220–229. DOI: 10.1016/j.jhazmat.2008.01.024.

13. Babel, S. & Kurniawan, T.A. Low-cost adsorbents for heavy metals uptake from contaminated water: A review. *J. Hazard. Mater*. 97 (2003) 219–243. DOI: 10.1016/S0304-3894(02)00263-7.

14. Bhattacharyya, K.G. & Sen Gupta, S., Adsorption of a few heavy metals on natural and modified kaolinite and montmorillonite: A review. *Adv. Colloid Interface Sci.* 140 (2008) 114–131. DOI: 10.1016/j.cis.2007.12.008.

15. Shen, J., Li, Z., nan Wu, Y., Zhang, B. & Li, F., Dendrimer-based preparation of mesoporous alumina nanofibers by electrospinning and their application in dye adsorption. *Chem. Eng. J*. 264 (2015) 48–55. DOI: 10.1016/j.cej.2014.11.069.

16. Song, L., Huo, J., Wang, X., Yang, F., He, J., Li, C. Phosphate adsorption by a Cu(II)-loaded polyethersulfone--type metal affinity membrane with the presence of coexistent ions. *Chem. Eng. J*. 284 (2016) 182–193. DOI: 10.1016/j.cej.2015.08.146.

17. Lalia, B.S., Kochkodan, V., Hashaikeh, R., Hilal, N. A review on membrane fabrication: Structure, properties and performance relationship, Desalination. 326 (2013) 77–95. DOI: 10.1016/j.desal.2013.06.016.

18. Huang, Z.M., Zhang, Y.Z., Kotaki, M., Ramakrishna, S. A review on polymer nanofibers by electrospinning and their applications in nanocomposites, Compos. Sci. Technol. 63 (2003) 2223–2253. DOI: 10.1016/S0266-3538(03)00178-7.

19. Ma, Z., Masaya, K. & Ramakrishna, S. Immobilization of Cibacron blue F3GA on electrospun polysulphone ultra-fine fiber surfaces towards developing an affinity membrane for albumin adsorption. *J. Memb. Sci*. 282 (2006) 237–244. DOI: 10.1016/j.memsci.2006.05.027.

20. Wu, J., Wang, N., Zhao, Y. & Jiang, L. Electrospinning of multilevel structured functional micro-/nanofibers and their applications. *J. Mater. Chem. A*. 1 (2013) 7290. DOI: 10.1039/c3ta10451f.

21. Ahmad, B., Stoyanov, S., Pelan, E., Stride, E. & Edirisinghe, M. Electrospinning of ethyl cellulose fibres with glass and steel needle configurations. *FOOD Res. Int*. 54 (2013) 1761–1772. DOI: 10.1016/j.foodres.2013.09.021.

22. Patil, S.S., Shedbalkar, U.U., Truskewycz, A., Chopade, B.A. & Ball, A.S. Nanoparticles for environmental clean-up: A review of potential risks and emerging solutions. *Environ. Technol. Innov*. 5 (2016) 10–21. DOI: 10.1016/j.eti.2015.11.001.

23. Steenkamp, G.C., Keizer, K., Neomagus, H.W.J.P. & Krieg, H.M. Copper(II) removal from polluted water with alumina/chitosan composite membranes. *J. Memb. Sci*. 197 (2002) 147–156. DOI: 10.1016/S0376-7388(01)00608-1.

24. Han, R., Zou, W., Zhang, Z., Shi, J., Yang, J. Removal of copper(II) and lead(II) from aqueous solution by manganese oxide coated sand. I. Characterization and kinetic study. *J. Hazard. Mater*. 137 (2006) 384–395. DOI: 10.1016/j.jhazmat.2006.02.021.

25. Wang, S.G., Gong, W.X., Liu, X.W., Yao, Y.W., Gao, B.Y., Yue, Q.Y. Removal of lead(II) from aqueous solution by adsorption onto manganese oxide-coated carbon nanotubes. *Sep. Purif. Technol*. 58 (2007) 17–23. DOI: 10.1016/j.seppur.2007.07.006.

26. Rahmani, A., Mousavi, H.Z., Fazli, M. Effect of nanostructure alumina on adsorption of heavy metals, Desalination. 253 (2010) 94–100. DOI: 10.1016/j.desal.2009.11.027.

27. Medina, M., Tapia, J., Pacheco, S., Espinosa, M., Rodriguez, R. Adsorption of lead ions in aqueous solution using silica-alumina nanoparticles, J. Non. Cryst. Solids. 356 (2010) 383–387. DOI: 10.1016/j.jnoncrysol.2009.11.032.

28. Hua, M., Zhang, S., Pan, B., Zhang, W., Lv, L. & Zhang, Q. Heavy metal removal from water/wastewater by nanosized metal oxides: A review. *J. Hazard. Mater*. 211–212 (2012) 317–331. DOI: 10.1016/j.jhazmat.2011.10.016.

29. Contreras-Bustos, R., Espejel-Ayala, F., Cercado-Quezada, B., Jiménez-Becerril, J. & Jiménez-Reyes, M. Adsorption of Zn2+ from solutions on manganese oxide obtained via ozone precipitation reaction. *Polish J. Chem. Technol*. 18 (2016) 46–50. DOI: 10.1515/pjct-2016-0008.

30. Gholami, A., Moghadassi, A.R., Hosseini, S.M., Shabani, S. & Gholami, F. Preparation and characterization of polyvi-

nyl chloride based nanocomposite nanofiltration-membrane modified by iron oxide nanoparticles for lead removal from water. *J. Ind. Eng. Chem.* 20 (2014) 1517–1522. DOI: 10.1016/j.jiec.2013.07.041.

31. Li, J., Shi, Y., Cai, Y., Mou, S., Jiang, G., Adsorption of di-ethyl-phthalate from aqueous solutions with surfactant--coated nano/microsized alumina. *Chem. Eng. J*. 140 (2008) 214–220. DOI: 10.1016/j.cej.2007.09.037.

32. Taylor, G. Electrically Driven Jets, Proc. R. Soc. London A. 313 (1969) 453–475. DOI: 10.1098/rspa.1969.0205.

33. Matthews, J.A., Wnek, G.E., Simpson, D.G., Bowlin, G.L. Electrospinning of collagen nanofibers, Biomacromolecules. 3 (2002) 232–238. DOI: 10.1021/bm015533u.

34. Foo, K.Y. & Hameed, B.H. Insights into the modeling of adsorption isotherm systems. *Chem. Eng. J*. 156 (2010) 2–10. DOI: 10.1016/j.cej.2009.09.013.

35. Sadeghi Pouya, E., Abolghasemi, H., Esmaieli, M., Fatoorehchi, H., Hashemi, S.J. & Salehpour, A. Batch adsorptive removal of benzoic acid from aqueous solution onto modified natural vermiculite: Kinetic, isotherm and thermodynamic studies. *J. Ind. Eng. Chem*. 31 (2015) 199–215. DOI: 10.1016/j.jiec.2015.06.024.

36. Alberti, G., Amendola, V., Pesavento, M. & Biesuz, R. Beyond the synthesis of novel solid phases: Review on modelling of sorption phenomena. *Coord. Chem. Rev*. 256 (2012) 28–45. DOI: 10.1016/j.ccr.2011.08.022.

37. C.H. Giles, D. Smith, A. Huitson, A general treatment and classification of the solute adsorption isotherm. I. Theoretical. *J. Colloid Interface Sci.* 47 (1974) 755–765. DOI: 10.1016/0021-9797(74)90252-5.

38. Hamdaoui, O. & Naffrechoux, E. Modeling of adsorption isotherms of phenol and chlorophenols onto granular activated carbon. Part I. Two-parameter models and equations allowing determination of thermodynamic parameters. *J. Hazard. Mater*. 147 (2007) 381–394. DOI: 10.1016/j.jhazmat.2007.01.021.

39. Sari, A. & Tuzen, M. Biosorption of total chromium from aqueous solution by red algae (Ceramium virgatum): Equilibrium, kinetic and thermodynamic studies. J. *Hazard. Mater*. 160 (2008) 349–355. DOI: 10.1016/j.jhazmat.2008.03.005.

40. Choong, C.E., Ibrahim, S., Yoon, Y. & Jang, M., Removal of lead and bisphenol A using magnesium silicate impregnated palm-shell waste powdered activated carbon: Comparative studies on single and binary pollutant adsorption. Ecotoxicol. Environ. Saf. 148 (2018) 142–151. DOI: 10.1016/j.ecoenv.2017.10.025.

41. Bediako, J.K., Reddy, D.H.K., Song, M.H., Wei, W., Lin, S. & Yun, Y.S., Preparation, characterization and lead adsorption study of tripolyphosphate-modified waste Lyocell fibers. *J. Environ. Chem. Eng.* 5 (2017) 412–421. DOI: 10.1016/j.jece.2016.12.022.

42. Georgescu, A.M., Nardou, F., Zichil, V. & Nistor, I.D. Adsorption of lead(II) ions from aqueous solutions onto Cr--pillared clays, Appl. Clay Sci. (2017) 0–1. DOI: 10.1016/j.clay.2017.10.031.

43. Tabesh, S., Davar, F. & Loghman-Estarki, M.R. Preparation of γ-Al_2O_3 nanoparticles using modified sol-gel method and its use for the adsorption of lead and cadmium ions, Elsevier B.V., 2017. DOI: 10.1016/j.jallcom.2017.09.246.

44. Vijayalakshmi, K., Devi, B.M., Latha, S., Gomathi, T., Sudha, P.N., Venkatesan, J. & Anil, S. Batch adsorption and desorption studies on the removal of lead (II) from aqueous solution using nanochitosan/sodium alginate/microcrystalline cellulose beads. *Int. J. Biol. Macromol.* 104 (2017) 1483–1494. DOI: 10.1016/j.ijbiomac.2017.04.120.

45. Zhang, Y., Cao, B., Zhao, L., Sun, L., Gao, Y., Li, J. & Yang, F. Biochar-supported reduced graphene oxide composite for adsorption and coadsorption of atrazine and lead ions. *Appl. Surf. Sci*. 427 (2018) 147–155. DOI: 10.1016/j.apsusc.2017.07.237.

46. Gomez-Gonzalez, R., Cerino-Córdova, F.J., Garcia-León, A.M., Soto-Regalado, E., Davila-Guzman, N.E. & Salazar-Rabago, J.J. Lead biosorption onto coffee grounds: Comparative analysis of several optimization techniques using equilibrium adsorption models and ANN. *J. Taiwan Inst. Chem. Eng*. 68 (2016) 201–210. DOI: 10.1016/j.jtice.2016.08.038.

47. Wang, C., Fan, X., Wang, P., Hou, J., Ao, Y. & Miao, L. Adsorption behavior of lead on aquatic sediments contaminated with cerium dioxide nanoparticles. *Environ. Pollut*. 219 (2016) 416–424. DOI: 10.1016/j.envpol.2016.05.025.

48. Sing, K.S.W. Reporting physisorption data for gas/solid systems with special reference to the determination of surface area and porosity. *Pure Appl. Chem*. 54 (1982) 2201–2218. DOI: 10.1351/pac198557040603.

49. Liu, D., Que, G.H., Wang, Z.X., Yan, Z.F. In situ FT-IR study of CO and H_2 adsorption on a Pt/Al_2O_3 catalyst, Catal. Today. 68 (2001) 155–160. DOI: 10.1016/S0920-5861(01)00306-6.

50. Alvar, E.N., Rezaei, M. & Alvar, H.N. Synthesis of mesoporous nanocrystalline $MgAl_2O_4$ spinel via surfactant assisted precipitation route. Powder Technol. 198 (2010) 275–278. DOI: 10.1016/j.powtec.2009.11.019.

51. Kao, L.H. & Hsu, T.C. Silica template synthesis of ordered mesoporous carbon thick films with 35-nm pore size from mesophase pitch solution. Mater. Lett. 62 (2008) 695–698. DOI: 10.1016/j.matlet.2007.06.034.

52. Mosquera, M.J., d. los Santos, D.M., Valdez-Castro, L. & Esquivias, L. New route for producing crack-free xerogels: Obtaining uniform pore size. J. Non. Cryst. Solids. 354 (2008) 645–650. DOI: 10.1016/j.jnoncrysol.2007.07.095.

53. Wang, S., Lu, Z., Wang, D., Li, C., Chen, C. & Yin, Y. Porous monodisperse V_2O_5 microspheres as cathode materials for lithium-ion batteries. *J. Mater. Chem*. 21 (2011) 6365. DOI: 10.1039/c0jm04398b.

54. Gupta, S., Ramamurthy, P.C. & Madras, G. Synthesis and characterization of flexible epoxy nanocomposites reinforced with amine functionalized alumina nanoparticles: a potential encapsulant for organic devices. Polym. Chem. 2 (2011) 221. DOI: 10.1039/c0py00270d.

55. Tangsir, S., Hafshejani, L.D., Lähde, A., Maljanen, M., Hooshmand, A., Naseri, A.A., Moazed, H., Jokiniemi, J. & Bhatnagar, A., Water defluoridation using Al_2O_3 nanoparticles synthesized by flame spray pyrolysis (FSP) method. Chem. Eng. J. 288 (2016) 198–206. DOI: 10.1016/j.cej.2015.11.097.

56. Huang, L.Y., Yu, D.G., Branford-White, C. & Zhu, L.M. Sustained release of ethyl cellulose micro-particulate drug delivery systems prepared using electrospraying. *J. Mater. Sci.* 47 (2012) 1372–1377. DOI: 10.1007/s10853-011-5913-x.

57. Es-haghi, H., Mirabedini, S.M., Imani, M. & Farnood, R.R., Preparation and characterization of pre-silane modified ethyl cellulose-based microcapsules containing linseed oil, Colloids Surfaces A Physicochem. Eng. Asp. 447 (2014) 71–80. DOI: 10.1016/j.colsurfa.2014.01.021.